at the highest E fields, thus permitting the use of thicker samples.

We have measured data storage error rates in a holographic optical storage test stand (*27–29*). Here a coherent 676-nm, data-containing object beam is intersected with a plane-wave reference beam in the PR sample (90% 2BNCM, 9.7% PMMA, 0.3% TNF) and a hologram is formed. A portion of a 64-kbit random data page is shown in Fig. 2. The size of each data bit on the mask was 18 μm by 18 μm, and each bit was surrounded by a 9 μm thick, opaque boarder with an overall pitch of 36 μm by 36 μm. The coherent object beam is passed through the data page mask containing the information as just described and focused on the sample to a 4-mm-diameter spot. The hologram is read back by illuminating the sample with only the reference beam and the reconstructed hologram recorded on a charge-coupled device (CCD) detector array. Experiments involved the storage, retrieval, and subsequent erasure of digital data pages with a data density of 0.5 Mbit/cm^2. For the amorphous glass system described here, single data pages could be stored and retrieved without error using only 1 part in 10^6 of the total dynamic recording range (that is, Δn range). Holograms were read back periodically at room temperature in air for up to 6 hours with no observable degradation in hologram quality or bit error rate.

The vanishingly small scattering levels in these glasses reduce the hologram efficiency required for error-free readout by a factor of 10 compared with polymeric systems studied previously. Of perhaps equal importance is the extremely large recording dynamic range available in these dihydropyridine systems. The overmodulation of the holographic efficiency, occurring at relatively small E fields (see Fig. 1), means that the smaller field can be applied to thicker samples, increasing the Bragg sensitivity, the number of holograms that can be multiplexed, and the overall hologram quality. In relation to existing polymeric PR systems, these organic glasses would appear to offer substantial advantages.

REFERENCES AND NOTES

1. P. Günter and J. P. Huignard, *Photorefractive Materials and Their Applications* (Springer, Berlin, 1988 and 1989), vols. 1 and 2.
2. M. Eich *et al.*, *J. Opt. Soc. Am. B* **6**, 1590 (1989); R. J. Twieg and C. W. Dirk, in *Science and Technology of Organic Thin Films for Waveguiding Nonlinear Optics*, F. Kajzar and J. Swalen, Eds. (Gordon and Breach, Newark, NJ, 1996).
3. A. Ashkin *et al.*, *Appl. Phys. Lett.* **9**, 72 (1966); F. S. Chen, *J. Appl. Phys.* **38**, 3418 (1967).
4. S. Ducharme, J. C. Scott, R. J. Twieg, W. E. Moerner, *Phys. Rev. Lett.* **66**, 1846 (1991).
5. W. E. Moerner and S. M. Silence, *Chem. Rev.* **94**, 127 (1994).
6. Y. Zhang, R. Burzynski, S. Ghosal, M. Casstevens, *Adv. Mater.* **8**, 111 (1996); L. Yu, W. K. Chan, Z. Peng, A. Gharavi, *Acc. Chem. Res.* **29**, 13 (1996).
7. M. Liphardt *et al.*, *Science* **263**, 367 (1994).
8. M. C. J. M. Donckers *et al.*, *Opt. Lett.* **18**, 1044 (1993).
9. O. Zobel, M. Eckl, P. Strohriegl, D. Haarer, *Adv. Mater.* **11**, 911 (1995).
10. K. Meerholtz, B. L. Volodin, Sandalphon, B. Kippelin, N. Peyghambarian, *Nature* **371**, 497 (1994).
11. K. Meerholz, Sandalphon, B. L. Volodin, B. Kippelin, N. Peyghambarian, *Conf. Lasers Electro-Opt. Tech. Dig.* **9**, 497 (1996).
12. C. Poga *et al.*, *Proc. Photo.-Opt. Instrum. Eng.* **2526**, 82 (1995).
13. A. M. Cox *et al.*, *Appl. Phys. Lett.* **68**, 2801 (1996).
14. W. E. Moerner, S. M. Silence, F. Hache, G. C. Bjorklund, *J. Opt. Soc. Am. B* **11**, 320 (1994).
15. R. Wortmann *et al.*, *J. Chem. Phys.*, in press.
16. S. R. Marder, D. N. Beratan, L.-T. Cheng, *Science* **252**, 103 (1991).
17. S. M. Silence *et al.*, *J. Phys. Chem.* **99**, 4096 (1995).
18. S. M. Silence, R. J. Twieg, G. C. Bjorklund, W. E. Moerner, *Phys. Rev. Lett.* **73**, 2047 (1994).
19. Y. Zhang, S. Ghosal, M. K. Casstevens, R. Burzynski, *Appl. Phys. Lett.* **66**, 256 (1995).
20. I. Belsky, H. Dodiuk, Y. Shvo, *J. Org. Chem.* **39**, 989 (1974).
21. W. E. Moerner *et al.*, *Proc. Soc. Photo-Opt. Instrum. Eng.* **1564**, 278 (1991).
22. C. A. Walsh and W. E. Moerner, *J. Opt. Soc. Am. B* **9**, 1642 (1992); *ibid.* **10**, 753 (1993).
23. B. L. Volodin *et al.*, *Opt. Lett.* **21**, 519 (1996).
24. F. S. Chen, J. T. LaMacchia, D. B. Frazer, *Appl. Phys. Lett.* **13**, 223 (1968).
25. J. F. Heanue, M. C. Bashaw, L. Hesselink, *Science* **265**, 749 (1994).
26. P. van Heerden, *Appl. Opt.* **2**, 393 (1963).
27. M.-P. Bernal *et al.*, *ibid.* **35**, 2360 (1996).
28. P. M. Lundquist *et al.*, *Opt. Lett.* **12**, 890 (1996).
29. C. Poga *et al.*, *Appl. Phys. Lett.* **69**, 1047 (1996).

30. We thank M.-P. Bernal, H. Coufal, R. K. Grygier, J. A. Hoffnagle, C. M. Jefferson, R. M. Macfarlane, R. M. Shelby, G. T. Sincerbox, P. Wimmer, and G. Wittmann for assistance in using the holographic optical storage test stand. Supported in part by ARPA contracts DAAB07-91-C-K767 and MDA972-94-20008.

9 August 1996; accepted 8 October 1996

Modulation of Insulin Activities by Leptin

Batya Cohen, Daniela Novick, Menachem Rubinstein*

Leptin mediates its effects on food intake through the hypothalamic form of its receptor OB-R. Variants of OB-R are found in other tissues, but their function is unknown. Here, an OB-R variant was found in human hepatic cells. Exposure of these cells to leptin, at concentrations comparable with those present in obese individuals, caused attenuation of several insulin-induced activities, including tyrosine phosphorylation of the insulin receptor substrate–1 (IRS-1), association of the adapter molecule growth factor receptor–bound protein 2 with IRS-1, and down-regulation of gluconeogenesis. In contrast, leptin increased the activity of IRS-1–associated phosphatidylinositol 3-kinase. These in vitro studies raise the possibility that leptin modulates insulin activities in obese individuals.

Leptin, an adipocyte-derived cytokine that regulates body weight, was identified by positional cloning of the murine *obese* (*ob*) gene (*1*) and was shown to affect both food intake and thermogenesis (*2*). High-affinity leptin-binding sites were detected in the choroid plexus, which led to identification of the leptin receptor OB-R (*3*). The known activities of leptin are mediated through the hypothalamic OB-R, but OB-R and OB-R variants derived from alternative splicing are expressed in other tissues, notably the kidney, lung, and liver (*3–5*). This receptor expression pattern suggests that, in addition to control of food intake and body heat, leptin may have other physiological functions. Although leptin is produced by adipocytes, the recent finding that excess fat correlates with high concentrations of leptin in serum (*6*), and the well-established linkage between obesity and insulin resistance (*7*), led us to explore the possibility that leptin may modulate insulin-regulated responses.

To test for possible effects of leptin on insulin-regulated responses, we looked for cell lines expressing a functional OB-R. Various human cell lines derived from liver, lung, and kidney were screened by reverse transcription–polymerase chain reaction (RT-PCR) with oligonucleotides corresponding to the region encoding the extracellular domain of human OB-R (huOB-R) (*3*). The human hepatocellular carcinoma cell lines HepG2 and Hep3B provided one PCR product whose identity with huOB-R mRNA was confirmed by DNA sequencing. Additional RT-PCR was done with primers corresponding to specific 3′ end regions of the four known splice variants of huOB-R. Only one splice variant, with a short cytoplasmic domain (the B219.3–OB-R mRNA) (*5*), was detected in HepG2 cells. The same product was obtained when RT-PCR was done with mRNA from human liver (Fig. 1A), and its identity was confirmed by sequencing. Northern blot anal-

Department of Molecular Genetics, The Weizmann Institute of Science, Rehovot 76100, Israel.

*To whom correspondence should be addressed. E-mail: lvrub@weizmann.weizmann.ac.il

ysis of RNA from human liver and HepG2 cells showed bands of indistinguishable size, albeit in different amounts (Fig. 1B). Two transcripts of 3 to 4 kb and 6 to 7 kb were obtained, in agreement with previous reports on liver transcripts (5). Two additional RNA molecules were detected, but they were too short to encode a transmembrane receptor.

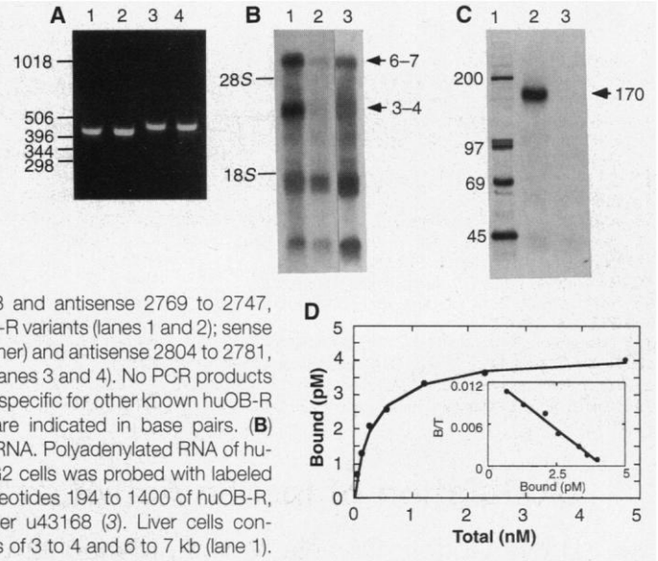

Fig. 1. Characterization of the leptin receptor OB-R and its mRNA in cells of hepatic origin. (**A**) RT-PCR of mRNA from human liver (lanes 1 and 3) and HepG2 cells (lanes 2 and 4). The following PCR primers, corresponding to B219.3–OB-R, GenBank accession number u52914 (*5*) were used: sense 2508 to 2538 and antisense 2769 to 2747, common to all known huOB-R variants (lanes 1 and 2); sense 2508 to 2538 (common primer) and antisense 2804 to 2781, specific for B219.3–OB-R (lanes 3 and 4). No PCR products were obtained with primers specific for other known huOB-R variants. Molecular sizes are indicated in base pairs. (**B**) Northern blot analysis of mRNA. Polyadenylated RNA of human liver and human HepG2 cells was probed with labeled DNA corresponding to nucleotides 194 to 1400 of huOB-R, GenBank accession number u43168 (*3*). Liver cells contained two major transcripts of 3 to 4 and 6 to 7 kb (lane 1). HepG2 cells (lane 2) contained transcripts of identical size, which are more visible when overexposed (lane 3). (**C**) Cross-linking of leptin to HepG2 cells results in a single 170-kD ligand-receptor complex. ^{125}I-leptin (*17*) was cross-linked to HepG2 cells (2×10^8 cells) in the absence (lane 2) or presence (lane 3) of excess unlabeled leptin. Cell extracts were immunoprecipitated with antibodies to leptin and analyzed by SDS–polyacrylamide gel electrophoresis (SDS-PAGE) and autoradiography. Molecular mass markers (lane 1) are indicated (in kilodaltons). (**D**) Binding of ^{125}I-leptin to HepG2 cells and Scatchard analysis (inset) of the saturation binding curve. Cells were incubated with increasing concentrations of ^{125}I-leptin (2×10^{17} decompositions per minute per mole). B/T, bound/total.

At the protein level, ligand-binding experiments revealed the presence of a functional OB-R in cells of hepatic origin. Cross-linking of ^{125}I-labeled leptin (15 kD) to HepG2 cells, followed by immunoprecipitation with antibodies to leptin, yielded a single 170-kD band, corresponding to the receptor-ligand complex (Fig. 1C). HepG2 cells bound ^{125}I-leptin in a saturable manner, and Scatchard analysis of the binding data revealed one class of high-affinity binding sites (5000 ± 400 sites per cell), with a dissociation constant (K_d) of 0.32 ± 0.038 nM (Fig. 1D). This K_d value is consistent with that reported for transfected cells expressing the hypothalamic OB-R (*3*). ^{125}I-leptin bound specifically to other cell types, including the rat hepatoma cell line H4-II-E, as determined by displacement with excess unlabeled ligand.

We next tested the effect of leptin on the profile of tyrosine-phosphorylated cellular proteins. HepG2 cells were treated with leptin for 5 to 30 min, and cellular proteins were analyzed by immunoblot analysis with antibodies to phosphotyrosine (anti-pTyr). The most profound effect of leptin was a reduction in the amount of a tyrosine-phosphorylated 185-kD protein, identified as the insulin receptor substrate–1 (IRS-1) by immunoprecipitation with a specific antibody. Pretreatment of HepG2 cells with leptin (3 or 60 nM) for 10 min down-regulated by a factor of 2 both the basal and the insulin-induced (100 nM, 1 min) tyrosine phosphorylation of IRS-1 (Fig. 2, A and B). Leptin reduced IRS-1 phosphorylation by a factor of 1.5 in H4-II-E cells (Fig. 2C). The effect of leptin on IRS-1 phosphorylation was specific, because tyrosine phosphorylation of the insulin receptor (IR) β chain was not reduced but rather was slightly increased (Fig. 2D).

Downstream signaling of IRS-1 is mediated by several associated proteins, including the adapter molecule growth factor receptor–bound protein 2 (GRB2) and phosphatidylinositol 3-kinase (PI 3-kinase) (*8*). We therefore tested the effect of leptin on the interaction of GRB2 and PI 3-kinase with IRS-1. Pretreatment of HepG2 cells with leptin reduced the basal and insulin-induced number of GRB2 binding sites in IRS-1 by factors of 1.4 and 1.8, respectively, as determined by the association of IRS-1 with a fusion protein consisting of glutathione-S-transferase (GST) and GRB2 (Fig. 3A). In addition, leptin reduced the basal and the insulin-induced binding of endogenous GRB2 to IRS-1 by a factor of 1.4, as determined by immunoprecipitation with anti-GRB2 and immunoblot analysis with

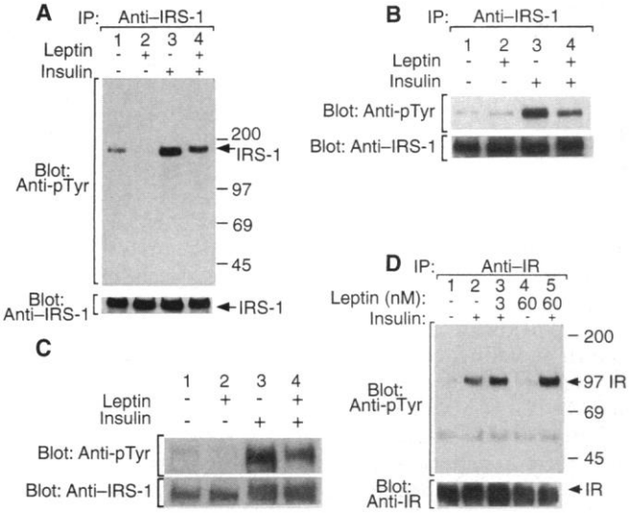

Fig. 2. Leptin down-regulates insulin-dependent tyrosine phosphorylation of IRS-1. (**A**) Serum-starved HepG2 cells were treated with leptin (60 nM, 10 min) and insulin (100 nM, 1 min) or with leptin followed by insulin (*18*). Cell extracts were immunoprecipitated (IP) with antibodies to IRS-1 and immunoblotted with anti-pTyr (Upstate Biotechnology) as described (*11, 19*). Control cells (lane 1) gave 361 ± 25 densitometric units. Leptin-treated cells (lane 2) gave 179 ± 21 units (probability $P < 0.05$, paired t test). Insulin-treated cells (lane 3) gave 1654 ± 126 units. Cells treated with leptin and insulin (lane 4) gave 642 ± 49 units ($P < 0.05$). The amount of IRS-1 was determined in the same blot by anti–IRS-1 (lower panel). (**B**) Same as (A), except that 3 nM leptin was used. (**C**) Rat H4-II-E cells were treated with leptin (3 nM) and insulin as in (A). Cell extracts were immunoblotted with anti-pTyr. Control cells (lane 1) gave 38 ± 6 units. Leptin-treated cells (lane 2) gave 32 ± 6 units. Insulin-treated cells (lane 3) gave 224 ± 18 units. Cells treated with leptin and insulin (lane 4) gave 148 ± 12 units, significantly lower ($P < 0.05$) than insulin-treated cells. (**D**) Extracts of HepG2 cells, treated as in (A), were immunoprecipitated with antibodies to human IR and immunoblotted with anti-pTyr. Control cells (lane 1) gave 183 ± 26 units. Insulin-treated cells (100 nM) (lane 2) gave 736 ± 122 units. Cells treated with leptin (3 nM) and insulin (100 nM) (lane 3) gave 880 ± 63 units. Cells treated with leptin (60 nM) alone (lane 4) gave 217 ± 16 units. Cells treated with leptin (60 nM) and insulin (100 nM) (lane 5) gave 1114 ± 175 units. The amount of IR was determined in the same blot by anti-IR (lower panel). In (A) and (D), molecular mass markers are shown on the right (in kilodaltons).

anti–IRS-1 (Fig. 3B). Similarly treated cells were analyzed for the association of PI 3-kinase with IRS-1. Here, both leptin and insulin increased the binding of PI 3-kinase to IRS-1 by threefold and fourfold, respectively, as determined by immunoprecipitation of cell extracts with antibodies to the p85 subunit of PI 3-kinase and immunoblot analysis with anti–IRS-1 (Fig. 4A). No additive increase of PI 3-kinase binding to IRS-1 was noticed when the cells were treated with both leptin and insulin (Fig. 4A). The leptin-induced increase in association of IRS-1 with PI 3-kinase was in apparent contrast with its attenuating effect on pTyr phosphorylation of IRS-1. We therefore measured the amount of PI 3-kinase catalytic activity in IRS-1 immunoprecipitates. Leptin and insulin increased the IRS-1–associated PI 3-kinase activity by twofold and fourfold, respectively, whereas a combination of the agents increased the activity by ninefold (Fig. 4B).

GRB2 and PI 3-kinase bind to different pTyr residues within IRS-1 (9). It is thus possible that most of the pTyr residues of IRS-1, including the GRB2 binding site (Tyr^{895}), are dephosphorylated in response to leptin, whereas the PI 3-kinase binding site (either Tyr^{608} or Tyr^{939}) may become phosphorylated. Such opposite effects of leptin may involve activation or recruitment of a specific protein tyrosine phosphatase and kinase. Alternatively, leptin may induce the phosphorylation of IRS-1 at serine residues, thereby inhibiting the IR kinase, as was reported in the case of tumor necrosis factor–α (TNF-α) (*10*). The effects of leptin on IRS-1 are not necessarily mediated through the IR kinase. Rather, they may result from an independent OB-R signaling cascade. Indeed, IRS-1 is not a specific substrate of the IR kinase. Rather, it is phosphorylated by additional growth factors and cytokines, including insulinlike growth factor–1, interferon-α, interleukin-4 (IL-4), and IL-9 (*11*, *12*). The rather short cytoplasmic domain of OB-R suggests the involvement of an accessory receptor subunit. Alternatively, it is possible that signaling in HepG2 cells is mediated by a longer form of OB-R that has not yet been identified.

We also investigated whether leptin affects glucose homeostasis in cell culture. Hepatic and renal gluconeogenesis is a major factor in maintaining glucose homeostasis. The rate-limiting enzyme of gluconeogenesis is phosphoenolpyruvate carboxykinase (PEPCK). This enzyme has no known allosteric control and is down-regulated by insulin at the transcriptional level. The rat hepatoma cell line H4-II-E has been used successfully to study the regulation of PEPCK expression, whereas HepG2 cells do not express PEPCK efficiently (*13*). The amount of PEPCK mRNA in H4-II-E cells treated first with N^6,2′-O-dibutyryladenosine 3′,5′-monophosphate (dibutyryl cAMP) and then with insulin was reduced by a factor of 4.8 compared to cells treated with dibutyryl cAMP alone. Incubation of

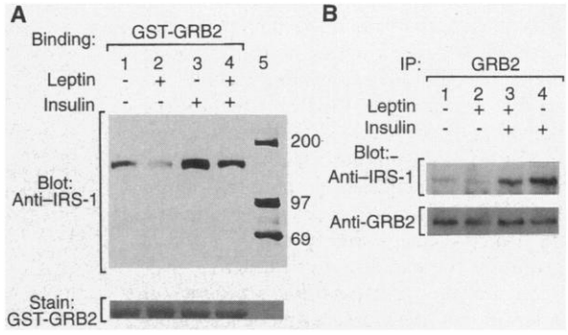

Fig. 3. Leptin attenuates the association of GRB2 with IRS-1. HepG2 cells were treated as in Fig. 2A. (**A**) Cell extracts were bound to GST-GRB2 fusion protein and glutathione-agarose, subjected to SDS-PAGE, and immunoblotted with anti–IRS-1 (*20*) followed by densitometry. Constitutive binding of IRS-1 to GST-GRB2 (257 ± 36 arbitrary units) was seen in control cells (lane 1). Leptin reduced this binding to 181 ± 23 units (lane 2). The number of GRB2 binding sites of IRS-1 in insulin-treated cells (626 ± 59 units, lane 3) was reduced to 353 ± 41 ($P < 0.02$) units upon treatment with leptin (lane 4). Molecular mass markers (lane 5) are indicated (in kilodaltons). The same amount of GST-GRB2 fusion protein was present in each lane, as shown by Ponceau S staining of the nitrocellulose membrane (lower panel). (**B**) Extracts were immunoprecipitated (IP) with polyclonal anti-GRB2 (Santa Cruz Biotechnology) and immunoblotted with anti–IRS-1 (upper panel). The amount of basal GRB2-associated IRS-1 (118 ± 16 units, lane 1) was decreased by leptin to 84 ± 12 units ($P < 0.08$, lane 2). The insulin-induced amount of GRB2-associated IRS-1 (327 ± 49 units, lane 4) was reduced to 228 ± 27 units ($P < 0.05$, lane 3). The amount of GRB2 was determined with anti-GRB2 (lower panel).

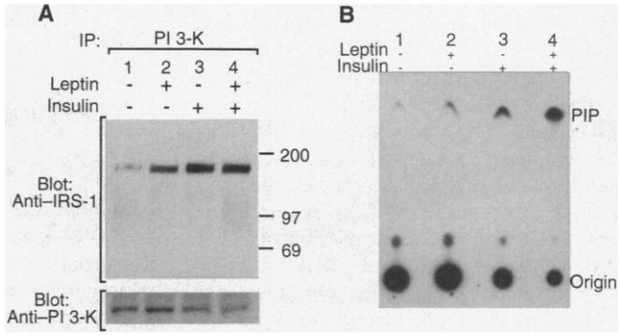

Fig. 4. Leptin increases the association of PI 3-kinase (PI 3-K) with IRS-1 and its activity. (**A**) HepG2 cells were treated as in Fig. 2A. Cell extracts were immunoprecipitated (IP) with polyclonal anti–PI 3-kinase (p85, Upstate Biotechnology) and immunoblotted with anti–IRS-1 (upper panel). The basal amount of PI 3-kinase, associated with IRS-1 (78 ± 7 units, lane 1), was increased both by leptin (240 ± 21 units, $P < 0.002$, lane 2) and by insulin (310 ± 28 units, $P < 0.001$, lane 3) as well as by treatment with both leptin and insulin (299 ± 26 units, lane 4). The amount of PI 3-kinase was determined with anti–PI 3-kinase (lower panel). Molecular mass markers are shown on the right (in kilodaltons). (**B**) HepG2 cells were treated as in Fig. 2A. Cell extracts were immunoprecipitated with polyclonal anti–IRS-1 and the immunoprecipitates were analyzed for in vitro PI 3-kinase activity (*11*). The basal level of IRS-1–associated PI 3-kinase activity, as determined by formation of phosphatidylinositol 4-phosphate (PIP; 740 ± 70 densitometric units, lane 1) was increased by leptin to 1583 ± 115 units ($P < 0.003$, lane 2) and by insulin to 2830 ± 231 units ($P < 0.005$, lane 3). Combined treatment with leptin and insulin increased the activity to 7030 ± 577 units ($P < 0.006$, lane 4).

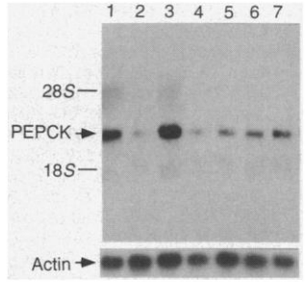

Fig. 5. Leptin up-regulates PEPCK expression. Serum-starved rat hepatoma H4-II-E cells (*13*) were pretreated with dibutyryl cAMP (0.5 mM, 3 hours) followed by treatment with leptin and insulin as in Fig. 2A. Northern blot analysis was done on cytoplasmic RNA with a DNA probe corresponding to rat PEPCK mRNA (positions 1364 to 1869 from the ATG start site). The amount of cytoplasmic PEPCK mRNA (arrow) in cells treated with insulin (10 nM, 2 hours) was reduced by a factor of 4.8 to 8.6 (333 ± 22 densitometric units, $P < 0.0001$, lane 2) compared with control cells or leptin-treated (60 nM, 2 hours) cells (1588 ± 121 and 2860 ± 244 units, lanes 1 and 3, respectively). Pretreatment of cells with leptin (3 nM) for 0.5, 1, or 2 hours, followed by treatment with insulin (10 nM, 2 hours), partially reversed the insulin-induced down-regulation of PEPCK mRNA expression (309 ± 21 units, lane 4; 480 ± 35 units, $P < 0.05$, lane 5; 585 ± 36 units, $P < 0.005$, lane 6). Pretreatment with 60 nM leptin for 1 hour, followed by treatment with insulin (10 nM, 2 hours) gave 741 ± 66 units ($P < 0.005$, lane 7). The same amount of RNA was present in each lane, as shown by reblotting the membrane with a probe corresponding to rat actin mRNA (positions 1670 to 2452 of the rat actin gene, lower panel).

the cells with leptin for 1 to 2 hours before addition of insulin partially reversed the down-regulating effect of insulin on PEPCK expression (Fig. 5). This observation is in contrast with the leptin-induced increase in PI 3-kinase activity obtained in HepG2 cells. Furthermore, the kinetics of the effect of leptin on PEPCK expression excludes its possible mediation by GRB2. It is therefore likely that leptin affects PEPCK gene expression by an as yet unknown pathway. On the basis of these results, we propose that leptin may affect gluconeogenesis, at least in the H4-II-E cell line, by attenuating the effect of insulin on the expression of PEPCK.

Several mouse strains that are deficient in leptin or OB-R serve as models for obesity, insulin resistance, and non-insulin–dependent diabetes mellitus (*1*, *4*, *14*). Therefore, it appears that excess leptin, as well as a complete absence of leptin, may impair some insulin responses, although not necessarily by the same mechanism. In the absence of leptin, other obesity-related factors may attenuate insulin responses. One such factor is TNF-α, which is overexpressed in adipocytes of obese animals. TNF-α down-regulates insulin-induced phosphorylation of IRS-1 and reduces expression of the insulin-dependent glucose transporter Glut4 (*10*, *15*).

Tyrosine phosphorylation of IRS-1 by the IR kinase is a key step in the IR signaling cascade, and GRB2 further mediates parts of this cascade (*8*, *16*). Therefore, the leptin-induced dephosphorylation of IRS-1 and its dissociation from GRB2 indicate that leptin may antagonize some functions of insulin. Although insulin resistance is poorly understood, it probably results from a combination of several factors and processes. Our finding that leptin attenuates some insulin-induced signals in hepatic cell lines, and the reports of increased serum leptin in obesity, warrants further studies on the possible role of leptin in obesity-associated insulin resistance.

REFERENCES AND NOTES

1. Y. Zhang *et al.*, *Nature* **372**, 425 (1994).
2. M. A. Pelleymounter *et al.*, *Science* **269**, 540 (1995); J. L. Halaas *et al.*, *ibid.*, p. 543; L. A. Campfield, F. J. Smith, Y. Guisez, R. Devos, P. Burn, *ibid.*, p. 546; D. S. Weigle *et al.*, *J. Clin. Invest.* **96**, 2065 (1995); S. Collins *et al.*, *Nature* **380**, 677 (1996).
3. L. A. Tartaglia *et al.*, *Cell* **83**, 1263 (1995).
4. G. H. Lee *et al.*, *Nature* **379**, 632 (1996).
5. J. A. Cioffi *et al.*, *Nature Med.* **2**, 585 (1996).
6. F. Lonnqvist, P. Arner, L. Nordfors, M. Schalling, *ibid.* **1**, 950 (1995); M. Maffei *et al.*, *ibid.*, p. 1155; R. C. Frederich *et al.*, *ibid.*, p. 1311; R. V. Considine *et al.*, *N. Engl. J. Med.* **334**, 292 (1996).
7. J. P. Felber and A. Golay, *Metabolism* **44** (suppl. 2), 4 (1995).
8. B. Cheatham and C. R. Kahn, *Endocrinol. Rev.* **16**, 117 (1995).
9. X. J. Sun, D. L. Crimmins, M. G. Myers Jr., M. Miralpeix, M. F. White, *Mol. Cell. Biol.* **13**, 7418 (1993); E. Y. Skolnik *et al.*, *EMBO J.* **12**, 1929 (1993).
10. G. S. Hotamisligil *et al.*, *Science* **271**, 665 (1996).
11. M. G. Myers Jr. *et al.*, *Endocrinology* **132**, 1421 (1993).
12. T. G. Yin, M. L. S. Tsang, Y. C. Yang, *J. Biol. Chem.* **269**, 26614 (1994); T. G. Yin *et al.*, *ibid.* **270**, 20497 (1995); S. Uddin *et al.*, *ibid.*, p. 15938; A. Pernis *et al.*, *Proc. Natl. Acad. Sci. U.S.A.* **92**, 7971 (1995).
13. D. Granner, T. Andreone, K. Sasaki, E. Beale, *Nature* **305**, 549 (1983); L. Xing and P. G. Quinn, *Mol. Endocrinol.* **7**, 1484 (1993).
14. H. Chen *et al.*, *Cell* **84**, 491 (1996); S. C. Chua Jr. *et al.*, *Science* **271**, 994 (1996).
15. R. Feinstein, H. Kanety, M. Z. Papa, B. Lunenfeld, A. Karasik, *J. Biol. Chem.* **268**, 26055 (1993); G. S. Hotamisligil, A. Budavari, D. Murray, B. M. Spiegelman, *J. Clin. Invest.* **94**, 1543 (1994); G. S. Hotamisligil and B. M. Spiegelman, *Diabetes* **43**, 1271 (1994); H. Kanety, R. Feinstein, M. Z. Papa, R. Hemi, A. Karasik, *J. Biol. Chem.* **270**, 23780 (1995).
16. M. G. Myers Jr. and M. F. White, *Diabetes* **42**, 643 (1993); M. G. Myers Jr., X. J. Sun, M. F. White, *Trends Biochem. Sci.* **19**, 289 (1994); M. G. Myers Jr. *et al.*, *Mol. Cell. Biol.* **14**, 3577 (1994); D. W. Rose, A. R. Saltiel, M. Majumdar, S. J. Decker, J. M. Olefsky, *Proc. Natl. Acad. Sci. U.S.A.* **91**, 797 (1994); H. Tamemoto *et al.*, *Nature* **372**, 182 (1994); E. Araki *et al.*, *ibid.*, p. 186; M. F. White and C. R. Kahn, *J. Biol. Chem.* **269**, 1 (1994).
17. Mouse leptin was purchased from Peprotech (Princeton, NJ). Antiserum to mouse leptin was obtained from a rabbit. For details on radioiodination, cross-linking, saturation binding, and Scatchard analysis, see B. Cohen, D. Novick, S. Barak, M. Rubinstein, *Mol. Cell. Biol.* **15**, 4208 (1995).
18. Serum-starved (24 hours) cells (4×10^7 cells) in Eagle's minimal essential medium were treated with insulin and leptin as indicated. Cells were washed three times with cold phosphate-buffered saline containing 1 mM Na_3VO_4 and lysed with 1 ml of cold lysis buffer [50 mM tris-HCl (pH 8.0), 1% Triton X-100, 1 mM Na_2 EDTA, 1 mM $MgCl_2$, 100 mM NaF, 1 mM phenylmethanesulfonyl fluoride, and aprotinin (5 μg/ml)]. Immunoprecipitation or precipitation with GST-GRB2 fusion protein was done on the clarified lysates. All autoradiograms were quantitated by densitometry and are averages of three independent experiments.
19. A. Kosaki, T. S. Pillay, L. Xu, N. J. Webster, *J. Biol. Chem.* **270**, 20816 (1995).
20. A. Ando *et al.*, *EMBO J.* **13**, 3033 (1994).

21. We thank S. Barak for technical help; H. S. Kim for help in Northern blot analysis; Y. Groner for valuable discussions; Y. Zick and H. Kanety for advice and for antibodies to IRS-1 and IR; Y. Yarden and G. Levkowitz for GST-GRB2 fusion protein; M. Walker, Y. Schechter, and D. Wallach for reviewing the manuscript; and M. Spigel for editorial assistance. M.R. holds the Edna and Maurice Weiss Chair of cytokine research.

19 July 1996; accepted 27 September 1996

From Peptide Precursors to Oxazole and Thiazole-Containing Peptide Antibiotics: Microcin B17 Synthase

Yue-Ming Li, Jill C. Milne, Lara L. Madison, Roberto Kolter, Christopher T. Walsh*

Escherichia coli microcin B17 is a posttranslationally modified peptide that inhibits bacterial DNA gyrase. It contains four oxazole and four thiazole rings and is representative of a broad class of pharmaceutically important natural products with five-membered heterocycles derived from peptide precursors. An in vitro assay was developed to detect heterocycle formation, and an enzyme complex, microcin B17 synthase, was purified and found to contain three proteins, McbB, McbC, and McbD, that convert 14 residues into the eight mono- and bisheterocyclic moieties in vitro that confer antibiotic activity on mature microcin B17. These enzymatic reactions alter the peptide backbone connectivity. The propeptide region of premicrocin is the major recognition determinant for binding and downstream heterocycle formation by microcin B17 synthase. A general pathway for the enzymatic biosynthesis of these heterocycles is formulated.

A growing number of peptide-based natural products have been found to contain thiazole and oxazole heterocyclic rings and exhibit significant antifungal, antibiotic, antitumor, and antiviral biological activities (*1*). The five molecules depicted in Fig. 1, bleomycin A_2, thiangazole, patellamide A, pristinamycin II_A, and thiostrepton, exemplify the patterns of such heterocycle occurrence in molecules of therapeutic interest. The antitumor antibiotic bleomycin uses the bithiazole moiety to intercalate into DNA (*2*). The tandem four-ring structure of thiangazole including the β-methyloxazoline provides potent antiviral activity against human immunodeficiency virus (*3*). Patellamides, cyclic octapeptides of marine origin, have antitumor properties (*4*). Thiostrepton, a protein synthesis inhibitor with four thiazole and one thiazoline ring is a signature secondary metabolite of *Streptomycetes* (*5*). Derivatives of pristinamycin (for example, RP59500) are currently in advanced clinical testing for combating vancomycin-resistant Gram-positive bacterial infections (*6*). The heterocyclic rings are likely to arise by cyclization of

Y.-M. Li, J. C. Milne, C. T. Walsh, Department of Biological Chemistry and Molecular Pharmacology, Harvard Medical School, Boston, MA 02115, USA.
L. L. Madison and R. Kolter, Department of Microbiology and Molecular Genetics, Harvard Medical School, Boston, MA 02115, USA.

*To whom correspondence should be addressed.